Check for updates

View Article Online
View Journal

Analyst

Accepted Manuscript

This article can be cited before page numbers have been issued, to do this please use: L. Qi, P. Parittothok, S. Sun, J. Wongwiwat, A. Thipayarat, W. Laiwattanapaisal and H. H. Yu, *Analyst*, 2026, DOI: 10.1039/D6AN00255B.

This is an Accepted Manuscript, which has been through the Royal Society of Chemistry peer review process and has been accepted for publication.

Accepted Manuscripts are published online shortly after acceptance, before technical editing, formatting and proof reading. Using this free service, authors can make their results available to the community, in citable form, before we publish the edited article. We will replace this Accepted Manuscript with the edited and formatted Advance Article as soon as it is available.

You can find more information about Accepted Manuscripts in the Information for Authors.

Please note that technical editing may introduce minor changes to the text and/or graphics, which may alter content. The journal's standard Terms & Conditions and the Ethical guidelines still apply. In no event shall the Royal Society of Chemistry be held responsible for any errors or omissions in this Accepted Manuscript or any consequences arising from the use of any information it contains.

ROYAL SOCIETY OF CHEMISTRY

rsc.li/analyst

View Article Online
DOI: 10.1039/D6AN00255B

Open Access Article. Published on 23 March 2026. Downloaded on 3/24/2026 12:02:26 AM.
This article is licensed under a Creative Commons Attribution-Non Commercial 3.0 Unported Licence.

Quantitative Analysis of Colorimetric Hydrogel/Paper Mini-Disk Arrays with a Handheld Wi-Fi Scanner

Lin Qi,[†,⊥] Pitipat Parittothok,[†,‡,⊥] Sophia Sun,[†] Jakrapop Wongwiwat,[‡] Aluck Thipayarat,[§] Wanida Laiwattanapaisal,[#] and Hua-Zhong Yu[†, #,*]

[†]*Department of Chemistry, Simon Fraser University, Burnaby, British Columbia V5A 1S6, Canada*

[‡]*Department of Mechanical Engineering, King Mongkut's University of Technology Thonburi, Bangkok 10140, Thailand*

[§] *Department Food Engineering, King Mongkut's University of Technology Thonburi, Bangkok 10140, Thailand*

[#] *Department of Clinical Chemistry, Chulalongkorn University, Bangkok 10330, Thailand*

* Corresponding author. E-mail: hogan_yu@sfu.ca

[⊥] These authors contributed equally to the work.

Abstract

Traditional quantitative colorimetric assays often rely on bulky laboratory instruments, such as UV-Vis spectrophotometers or microplate readers. While smartphone-based point-of-need (PON) tools have emerged as alternatives, they are frequently limited by ambient lighting variation and perspective distortion. To address these challenges, we developed a PON quantitative platform for colorimetric assays that integrates hydrogel (agarose based) coated filter paper as reaction "mini-disks", a handheld Wi-Fi scanner as the imaging tool, and a custom-designed app (universal for both smartphones and pads) for color analysis. Using two representative colorimetric assays, pH-differential colorimetry for anthocyanin and Ellman's assay for parathion methyl, we validated the performance of this new Wi-Fi scanning platform with conventional UV-Vis spectrophotometry analysis. The results demonstrate that this integrated Wi-Fi scanning protocol promises as a reliable, universal, low-cost, and convenient tool for on-site, quantitative colorimetric analysis in resource-limited settings.

KEYWORDS: colorimetric assay, point-of-need (PON) testing, handheld Wi-Fi scanner, hydrogel-paper mini disks, color analysis app

Analyst Accepted Manuscript

View Article Online
DOI: 10.1039/D6AN00255B

Open Access Article. Published on 23 March 2026. Downloaded on 3/24/2026 12:02:26 AM.
This article is licensed under a Creative Commons Attribution-Non Commercial 3.0 Unported Licence.

1. Introduction

Colorimetric assays are widely employed analytical techniques that detect target analytes via measurable changes in color. It typically arises from chemical or enzymatic reactions that convert a reactant or substrate into a chromogenic product with distinct colors.[1-4] In addition, nanomaterials such as gold and silver nanoparticles can serve as colorimetric reagents as well, which exhibit aggregation-dependent color changes in response to analyte interaction.[5-8] Colorimetric assays can achieve high sensitivity when UV–Vis spectrophotometers are used as detector; meanwhile, they offer distinct advantages over other instrumental techniques (e.g., gas/liquid chromatography and mass spectrometry), such as rapid response, ease of use, and high-throughput.[1,3,7,9] Furthermore, their integration with biosensing strategies, such as the use of chromogenic labels conjugated to biorecognition elements (e.g., antibodies, DNA) has enabled diverse applications in clinical diagnostics, food safety monitoring, and environmental analysis.[3,8-9]

As visible colors generated in colorimetric assays enable direct readout by naked eyes, they facilitate simple qualitative or semi-quantitative detection (e.g., through comparison with a reference color chart) without the need of any instruments or apparatus.[10] A well-established commercial example is the lateral flow immunochromatographic testing strip (e.g., pregnancy tests), in which the appearance of a colored band in the test region indicates the presence of the target analyte.[11-12] For quantitative analysis, UV/Vis absorbance measurements of the chromogenic products remain as the conventional method. According to the Beer's law, the absorbance of a colored compound is directly proportional to its concentration in solution. In practice, this involves the identification of the maximum absorption wavelength from the scanned spectrum, followed by the determination of absorbance values for a series of standard solutions with known analyte concentrations. A calibration curve is then constructed, enabling the determination of analyte concentrations in unknown sample by interpolation.[4, 13-14]

In recent years, smartphones with high-resolution cameras and fast data processing hardware have emerged as powerful platforms for quantitative colorimetric assays, their integration enables on-site, point-of-need, and real-time analysis in diverse settings, including household, clinic, and in-field environments.[15-24] By using this tool, assay results are captured as digital images, which can then be processed using commercial software (e.g., photoshop, ImageJ) or customized apps.[15,17,25-26] Color information is analyzed in grayscale or various color spaces (e.g., RGB or CMYK), and quantitative results are obtained by correlating the color intensity with the analyte concentration.[19,21,24] Moreover, with internet and cloud-based information systems smartphones allow easy data management, storage, remote access, sharing and delivery for further analysis. Besides smartphones, flatbed scanners have been explored as an alternative imaging tool for colorimetric assays; particularly handheld portable scanners offer advantages of low cost ($100-500 CAD depending on the exact model/brand and supplier), on-site use, and wireless connection (e.g., Wi-Fi, Bluetooth) with smartphones, laptops, and other electronic devices for data transfer and analysis.[27]

With the increasing adoption of smartphones and scanners as imaging tools for colorimetric assays, the devices to run such assay reactions have also evolved to be adaptable for PON testing. For example, filter paper is a popular substrate material that has been extensively explored for preparing colorimetric assays, as it is inexpensive, biocompatible, and easy to handle.[10, 28-31] Moreover, the highly porous and hydrophilic structure (a network of cross-linked cellulose fibers) of filter paper provides high permeability and strong capillary function, which enables spontaneous fluid flow without the need of external pumping.[10,28,31] Such a porous structure also allows for the preloading of reagents into filter paper and thereby simplify the detection process.[29] With wax printing, hydrophobic coatings, and UV lithography (with a patterned mask), reaction channels of specific dimensions and shapes can be created on filter paper.[26,29,32-34] Furthermore, the abundant functional groups of cellulose fibers (e.g., hydroxyl moieties) allow for diverse chemical and biological modifications, which significantly broadens its application scope of filter paper-based analytical

Analyst Accepted Manuscript

View Article Online
DOI: 10.1039/D6AN00255B

Open Access Article. Published on 23 March 2026. Downloaded on 3/24/2026 12:02:26 AM.
This article is licensed under a Creative Commons Attribution-NonCommercial 3.0 Unported Licence.

devices.[35] Besides filter paper, hydrogels with a water-swollen 3D polymer network structure have distinctive physical, chemical, mechanical and biological properties, which have also demonstrated similar advantages as the substrate for colorimetric assays.[36, 37] We and others recently developed novel pH testing strips by coating filter paper with agarose-based hydrogel, which results in enhanced loading capability and uniformity of chromogenic reagents (minimized "coffee-ring" effect), as well as improved color retention for quantitative analysis.[34,38]

In the present work, we explore the feasibility of creating an array of hydrogel-coated paper mini-disks, which would allow multiplex PON colorimetric detection, in conjunction with Wi-Fi scanning for data analysis. Specifically, the images of detection results are captured using a handheld Wi-Fi scanner, and the quantitation is performed via a customized app capable of analyzing color information in different color spaces (e.g., RGB, CMYK). To validate this new platform as a PON quantitative tool for colorimetric assays, we examined two diverse analytes (anthocyanin and parathion methyl), and compared their detection results to those obtained by conventional spectrophotometry measurements.

2. Results and discussion

2.1. Fabrication of hydrogel-paper mini-disk arrays for colorimetric assays

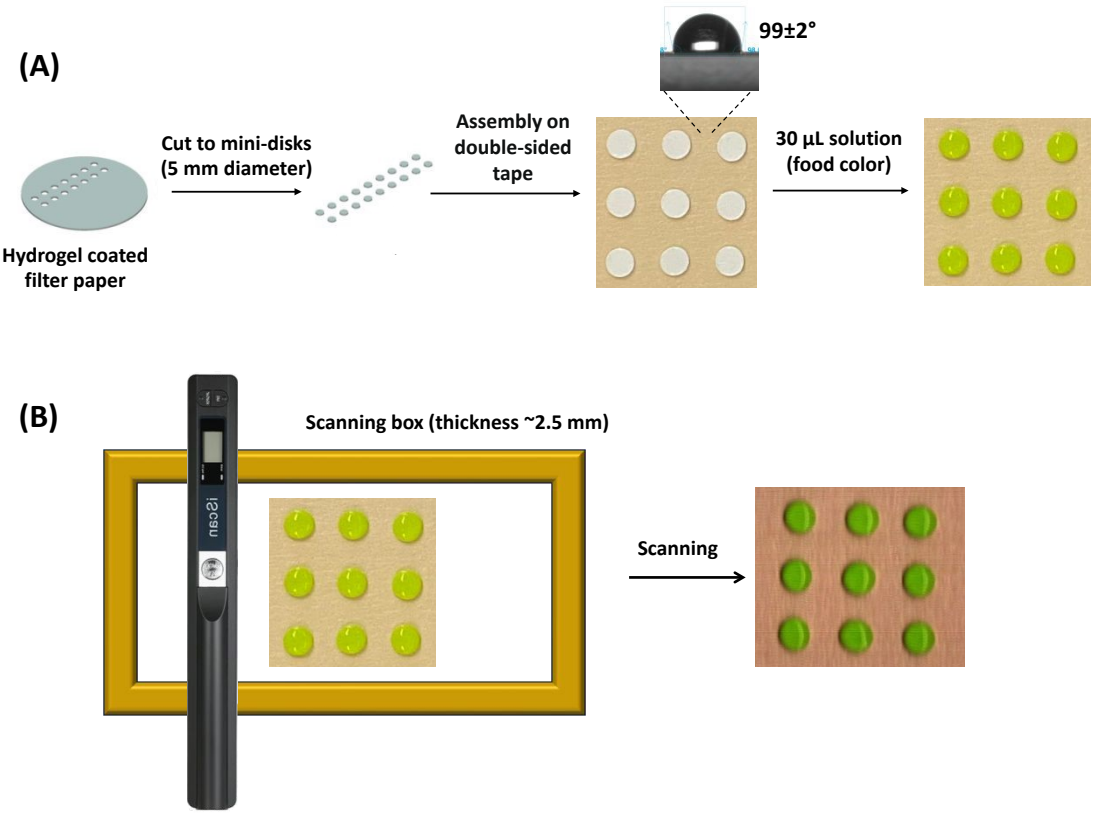

Fig. 1 (A) Cutting and assembling of hydrogel/paper mini-disk arrays. (B) Imaging the detection results by using a handheld Wi-Fi scanner (iScan).

The hydrogel (agarose-based) coated filter paper was fabricated by modifying a simple procedure reported in our previous work;[34] the details are provided in the experimental section. Different from the previous work, where agarose solution is mixed with colorimetric reagents (i.e., anthocyanin as a pH indicator) before coating, herein pure agarose solutions are used and the coated filter paper can be loaded with any colorimetric reagents depending on specific needs. As shown in Fig. 1A, the detection arrays are readily

Analyst Accepted Manuscript

View Article Online
DOI: 10.1039/D6AN00255B

prepared by machine-cutting the coated filter paper into mini-disks (5 mm diameter), which are well-aligned and assembled onto a double-sided tape. Since the tape is hydrophobic (water contact angle = 99 ± 2°), droplets of aqueous solutions (as much as 30 μL) can be well-held by the agarose-paper disk, which is easily adjusted by varying its diameter or even the shape.

To obtain the image of testing results, the mini-disk array is paced in a "imaging box" (3D-printed or using a stack of cardboard with a rectangular opening in the center). A handheld Wi-Fi scanner (iScan) is used to capture the image (1050 dpi) by moving it across the disk arrays (the built-in feedback mechanism of iScan scanners ensures the proper scanning speed of 2.5-3.0 cm/s for the selected resolution.[39] If the speed is too slow or too fast, warning symbols will appear on the device and the scan will stop automatically. The thickness of imaging box (~ 2.5 mm) ensures that the bottom of scanner (sensing area) does not touch the hydrogel-paper disks. After scanning, the image is automatically saved, which can be transferred to a smartphone or a pad via Wi-Fi. To analyze the color information, a custom-designed app (*ChromaDetect*) was used, which can run on any devices (smartphones, pads, or laptops) with a web browser (no OS restrictions) and supports uploading images in either PNG or JPEG format. With one or multiple pre-defined areas (a circle or rectangular region with adjustable coordinates and dimensions), the app is able to analyze color information (based on either RGB or CMYK color space) for each pixel and provide average and standard deviation values as outputs. In addition, a linear calibration equation (with fitted slope and intercept values) can be created, which enables the calculation of analyte concentration based on normalized color intensity. The results determined by this app can be exported to Excel sheets (xlsx) for further analysis if preferred. The original code of this app and the screenshot of its interface are provided in the Supporting Information.

2.2. Wi-Fi scanning pH-differential colorimetric assay for the quantitation of anthocyanins

We first validated this new analytical platform with a pH-differential colorimetric assay for anthocyanin (a class of water-soluble natural pigment that is widely used in food industry and has important nutritional value as antioxidants).[39-40] Developed by Sondheimer and Kertesz in 1948 and officially adopted by the Association of Official Agricultural Chemists (AOAC) since 2005,[41-42] the pH differential colorimetric assay we have performed is the standard protocol for monitoring anthocyanin levels in agricultural products. The major species of anthocyanin, Cyanidian-3-O-glucoside (> 50%), was particularly used in this study as the standard analyte for the quantitative detection as described below.

The principle of this pH-differential colorimetric assay is based on the structural switch of anthocyanin (Cy3G) from a red-colored flavylium cation at pH < 2 environment to a pair of colorless, resonant structures (hemiketal and chalcone) at pH 4-5 via hydration and deprotonation processes (Fig. 2A); with such a differential approach (instead of monitoring color change at a single pH) the matrix effect can be minimized.[42] As such, we have firstly confirmed the sensing principle by measuring UV/vis spectra for different concentrations of anthocyanin (Cy3G) dissolved in pH 1.0 solution (0.1 M HCl) and pH 4.5 buffer (NaAc/HAc). As shown in Fig. 2B and 2C, strong absorbance peaks are observed at pH 1.0, which correspond to the fully delocalized π-conjugation of flavylium cation; in contrast, much weaker absorbance was observed at pH 4.5. For example, the absorbance with a concentration of 80 mg/L is less than 0.1, which is over 1.5 at pH 1.0. This is the result of the disrupted π-conjugation by hydration and deprotonation process (Fig. 2A).

Open Access Article. Published on 23 March 2026. Downloaded on 3/24/2026 12:02:26 AM.
This article is licensed under a Creative Commons Attribution-Non Commercial 3.0 Unported Licence.
Analyst Accepted Manuscript

View Article Online
DOI: 10.1039/D6AN00255B

Open Access Article. Published on 23 March 2026. Downloaded on 3/24/2026 12:02:26 AM.
This article is licensed under a Creative Commons Attribution-NonCommercial 3.0 Unported Licence.

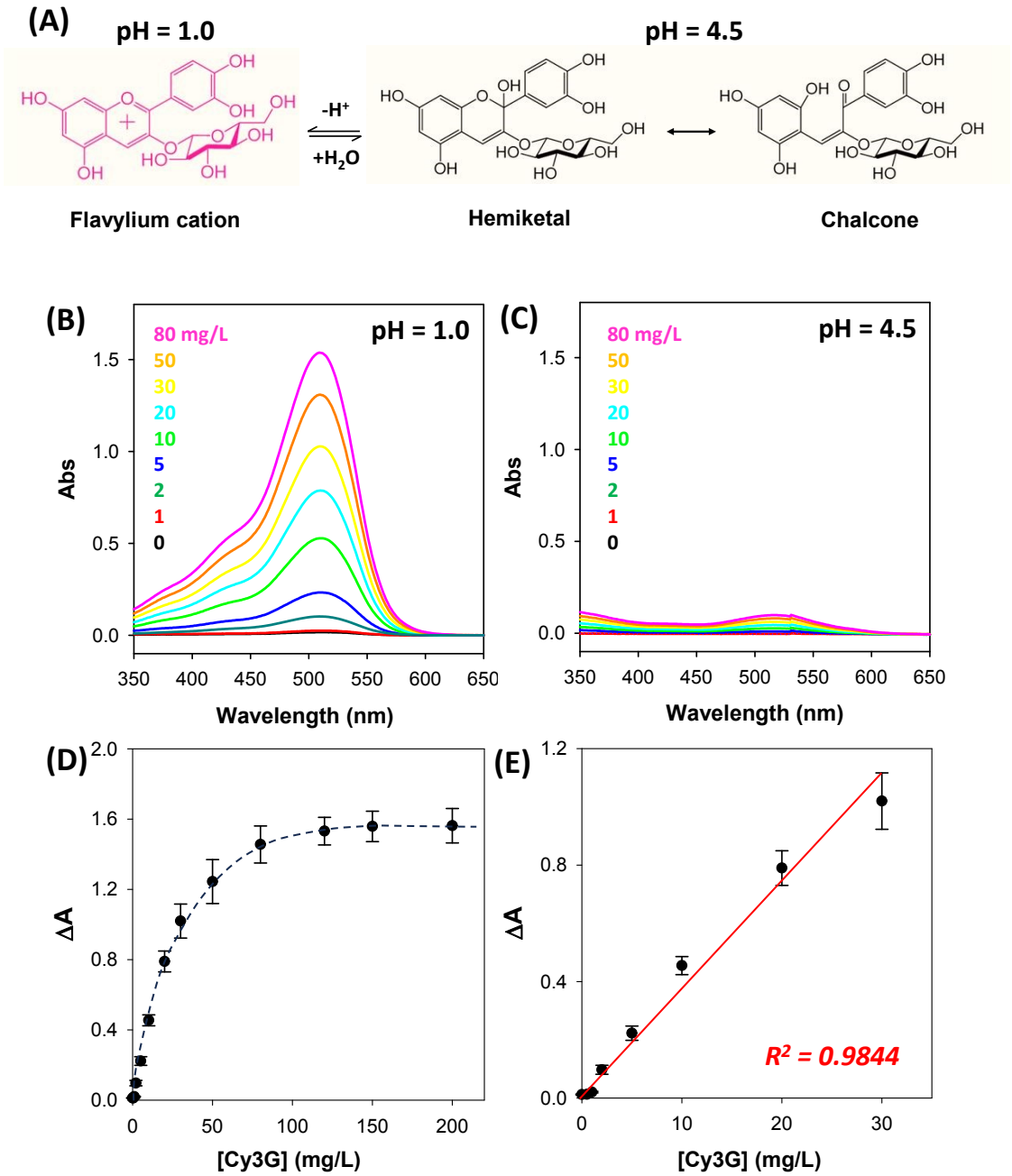

Fig. 2 (A) pH-dependent structural switching of anthocyanin (Cy3G). UV/vis spectra of different concentrations of anthocyanin (Cy3G) in (B) pH 1.0 solution and (C) pH 4.5 buffer. (D) Anthocyanin (Cy3G) calibration curve obtained by pH differential colorimetric assay ($\Delta A = A_{pH\ 1.0} - A_{pH\ 4.5}$). The dash line is to guide the eyes only. (E) Calibration curve from 0 to 30 mg/L (red line: the best linear fit). The error bars in (D) and (E) were obtained from at least three repeating experiments.

In accordance with previously reported protocol,[42] an anthocyanin (Cy3G) calibration curve can be established by plotting the difference in the maximum absorbance (ΔA) at 520 nm between pH 1.0 and pH 4.5 as a function of its concentration (i.e., $\Delta A = A_{pH\ 1.0} - A_{pH\ 4.5}$). As displayed in Fig. 2D, ΔA initially increases with increasing the concentration of anthocyanin (Cy3G), which becomes saturated over 100 mg/L. Indeed, a linear relationship can be established from 0 to 30 mg/L with $R^2 = 0.9844$ (Fig. 2E). Based on the best fitting equation, $\Delta A = 0.036 \pm 0.003\ [Cy3G] + 0.011 \pm 0.009$, the limit of detection (LOD), 0.75 ± 0.06 mg/L was determined from the slope (k) and the standard deviation (S_b) of the intercept ($3s_b/k$).

Analyst Accepted Manuscript

View Article Online
DOI: 10.1039/D6AN00255B

Open Access Article. Published on 23 March 2026. Downloaded on 3/24/2026 12:07:26 AM.
This article is licensed under a Creative Commons Attribution-Non Commercial 3.0 Unported Licence.

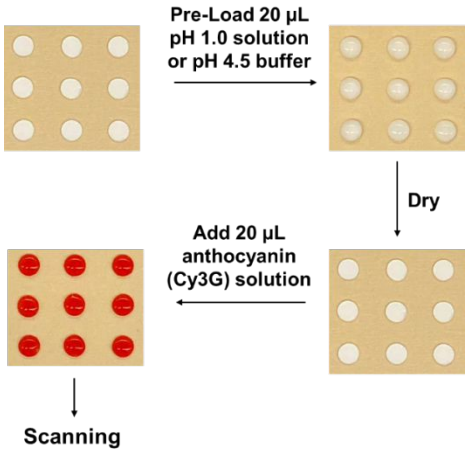

Fig. 3 Performing pH-differential colorimetric assay of anthocyanin (Cy3G) on a hydrogel-paper disk array.

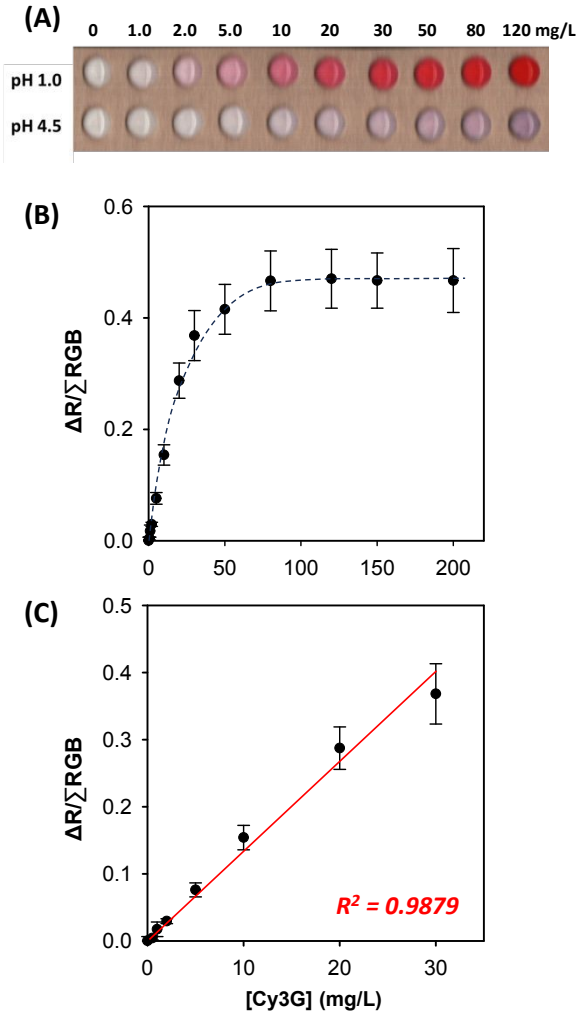

Fig. 4 (A) Scanned image of pH-differential colorimetric assay disks for the anthocyanin quantitation with the corresponding concentration listed at top. (B) Differential red intensities ($\Delta R/\Sigma RGB = R/\Sigma RGB_{pH\ 1.0} - R/\Sigma RGB_{pH\ 4.5}$) as a function of the Cy3G concentration. The dash line is to guide the eyes only. (C) Linear calibration data from 0 to 30 mg/L (red line: the best linear fit). The error bars in (B) and (C) were obtained from at least three repeating experiments.

As illustrated in Fig. 3, to perform anthocyanin colorimetric assay on hydrogel/paper disks, each disk is pre-loaded with 20 μL of pH 1.0 solution or pH 4.5 buffer. After drying, 20 μL Cy3G solution of different

Analyst Accepted Manuscript

View Article Online
DOI: 10.1039/D6AN00255B

Open Access Article. Published on 23 March 2026. Downloaded on 3/24/2026 12:02:26 AM.
This article is licensed under a Creative Commons Attribution-Non Commercial 3.0 Unported Licence.

concentrations was added to each paper disk, followed by scanning with the Wi-Fi scanner to obtain the results right away (as the color appears immediately).

Fig. 4A shows a scanned image of the anthocyanin detection results on two rows of hydrogel/paper diskdisks; it can be seen that with increasing concentrations of anthocyanin, the two rows of paper disks displayed varied colors: the top row (pre-loaded with pH 1.0 solution) changes from plain gray to bright red, while much less color changes were observed in the bottom row (pre-loaded with pH 4.5 buffer). By using the developed *ChromaDetect* app, the color generated on each paper disk was analyzed with RGB (Red, Green, and Blue) color space; and the difference in normalized red color intensity ($\Delta R/\Sigma RGB$, $\Sigma RGB = R + G + B$) obtained at pH 1.0 and pH 4.5 ($R/\Sigma RGB$ values at pH 1.0 and pH 4.5 are provided in Supporting Information, Fig. S4) is plotted against the concentration of anthocyanin. From the calibration curve, a bigger difference in $\Delta R/\Sigma RGB$ was observed with increasing concentrations of anthocyanin (Cy3G) standard, which essentially becomes saturated over 80 mg/L (Fig. 4B). In Fig. 4C, we have shown the best linear fit to the experimental data in the range of 0 to 30 mg/L, which yields an equation as: $\Delta R/\Sigma RGB = 0.012\pm0.002\ [Cy3G] + 0.0015\pm0.0033$, $R^2 = 0.9879$. The determined LOD (0.82 ± 0.11 mg/L) is indeed comparable with that of standard spectrophotometric results as described above. It is important to note that the sensing performance of the Wi-Fi scanning method does meet the industrial needs for food and beverage quality control (0.3-3 mg/L).[43]

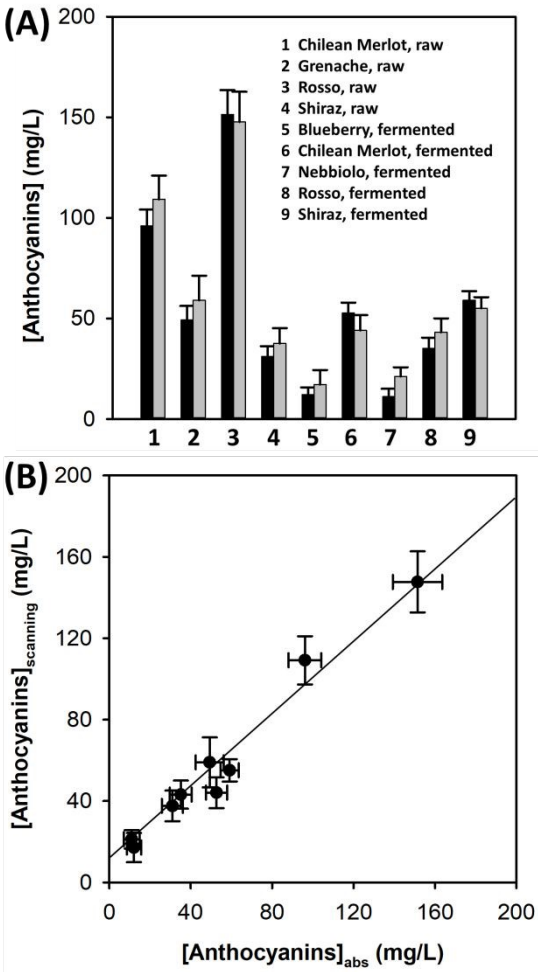

Fig. 5 (A) Comparison of the anthocyanin detection results by UV-vis spectrophotometry (black bars) and the Wi-Fi scanning method (gray bars). (B) Correlation between the anthocyanin concentrations determined via the spectrophotometry ($[\text{anthocyanins}]_{abs}$) and the Wi-Fi scanning method ($[\text{anthocyanins}]_{scanning}$). The solid line in (B) is the best linear regression curve. The error bars in (A) and (B) were obtained from at least three replicated experiments.

Analyst Accepted Manuscript

View Article Online
DOI: 10.1039/D6AN00255B

Open Access Article. Published on 23 March 2026. Downloaded on 3/24/2026 12:02:26 AM.
This article is licensed under a Creative Commons Attribution-Non Commercial 3.0 Unported Licence.

To further evaluate the practical application, we used above two methods to determine the concentration of anthocyanins in several beverages, which include four raw grape juices and five fermented wines (all samples were obtained from the production line of the Bayou Brewing Club, a sub-division of Laca Biotech Inc., Richmond, BC, Canada). The samples were diluted before testing. Based on their detection signals (ΔA at 512 nm or ΔR/RGB) and the linear calibration curves displayed in Fig. 2D and Fig. 2C, the concentration of anthocyanins in these samples were interpolated and summarized in Fig. 5A. It is evident that for most samples the quantitation results obtained by the two methods (gray bar: hydrogel/paper disk + Wi-Fi scanning; black bar: UV-vis absorbance measurements) are very close within experimental uncertainties (obtained from three repeating tests). For a more direct comparison, the determined concentrations of all samples ($[\text{anthocyanins}]_{\text{scanning}}$ vs. $[\text{anthocyanins}]_{\text{abs}}$) are plotted in Fig. 5B; the satisfactory linearity (R^2 = 0.9786) and close-to-unity slope (0.951) of the regression line further confirm the consistency between the conventional UV-vis spectrophotometry and our newly developed Wi-Fi scanning method.

2.3. Wi-Fi Scanning the Ellman's assay for the quantitation of parathion-methyl

Parathion-methyl is a highly toxic organophosphorus pesticide widely used in agricultural activities, its detection is critically important due to its severe health risks and environmental persistence. Monitoring of parathion-methyl level in food, water, and soil is essential to prevent acute poisoning, chronic exposure, and ecological damage.[44, 45] The gold standard method for detecting parathion-methyl is GC-MS, which provides high sensitivity (low μg/L for water samples and μg/kg for food and soil), selectivity, and reliable quantification of trace amounts in complex matrices.[46] Although less sensitive than GC-MS, the colorimetric detection of parathion-methyl based on Ellman's assay is simple, rapid, and inexpensive; moreover, it can be performed without extensive sample pretreatment, making it a useful tool for high-throughput screening and on-site detection.[47, 48] As illustrated in Fig. 6A, the principle of Ellman's assay is to measure the inhibition effect of parathion-methyl on the activity of acetylcholinesterase (ATChE). In this assay, the enzyme (ATChE) catalyzes the hydrolysis of acetylthiocholine (ATCh) at slightly alkaline conditions (pH = 7.5~8.0) to release thiocholine (TCh), which reacts with the Ellman's reagent, 5,5'-dithiobis-(2-nitrobenzoic acid) (DTNB) to form a yellow-colored product (TNB) with the maximum absorbance at 412 nm. Thus, the decreased color intensity or absorbance indicates the presence of parathion-methyl that inhibits the enzymatic activity of ATChE.

To start, we measured the UV/Vis spectra of the Ellman's assay solutions with and without adding parathion-methyl. As displayed in Fig. 6 (B), the standard Ellman's assay (containing ATChE, ATCh and DTNB, the reaction time was kept at 20 min) results in a strong absorption peak (red curve) with maximum wavelength at 412 nm; upon pre-incubating ATChE with of 5 μg/mL parathion-methyl, the absorption peak decrease significantly (blue curve), and a further decreased absorption peak is observed when parathion-methyl was increased to 20 μg/mL (green curve). As a control, no adsorption peak is observed when ATChE is not added to Ellman's assay (only ATCh and DTNB, black curve).

Analyst Accepted Manuscript

View Article Online
DOI: 10.1039/D6AN00255B

Open Access Article. Published on 23 March 2026. Downloaded on 3/24/2026 12:02:26 AM.
This article is licensed under a Creative Commons Attribution-Non Commercial 3.0 Unported Licence.

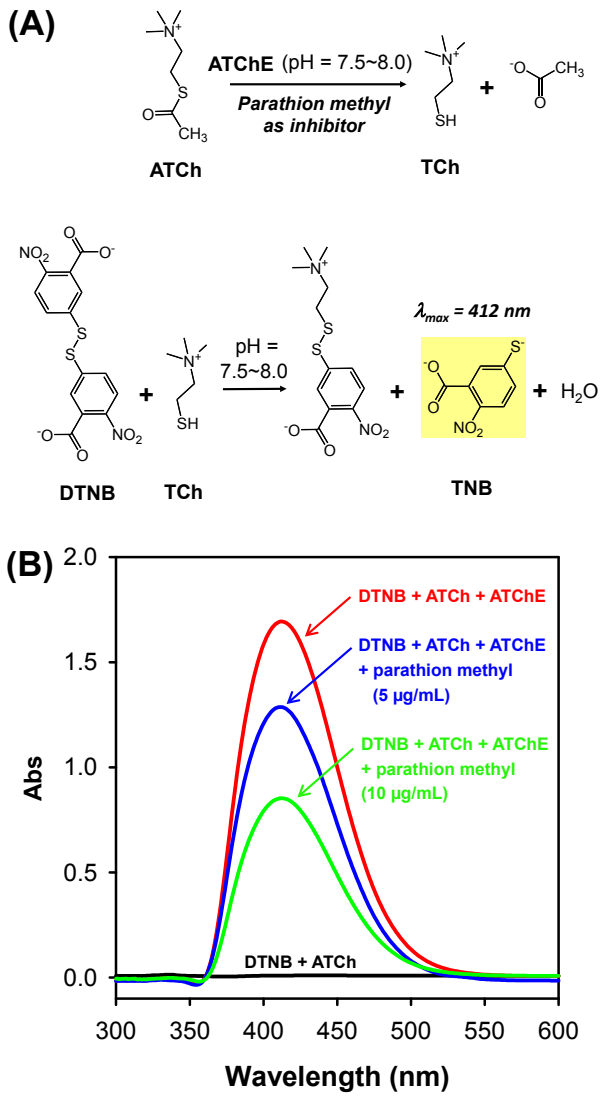

Fig. 6 (A) Reactions involved in the Ellman's assay for the colorimetric detection of parathion-methyl. (B) UV/Vis spectra recorded at 30 min of the Ellman's assay with 3 mM ATCh, 6 mM DTNB and 0.07 μg/mL ATChE. The ATChE solution is pre-incubated together with 0 μg/mL (red curve), 5 μg/mL (blue curve) and 20 μg/mL parathion methyl (green curve). The black curve is the UV/vis spectrum of 3 mM ATCh and 6 mM DTNB only (No ATChE added).

Similar to the procedure depicted in Fig. 3, to perform the Ellman's assay on hydrogel-paper disk arrays, the "empty" disk is pre-loaded with 20 μL solution of ATCh and DTNB mixture (1.0 mg/mL and 2.5 mg/mL respectively, dissolved in PB buffer, pH = 7.5). After drying, 20 μL solution of ATChE (pre-incubated with different concentrations of parathion-methyl at 37°C for 1h in PB buffer, pH = 7.5) was added to each of the assay disk, followed by monitoring the color change and Wi-Fi scanning to obtain the results.

Different from the anthocyanin colorimetric detection, for which the color changes immediately like a pH indicator,[39] the colorimetric detection of parathion methyl depends on an enzymatic reaction and produces a "signal-off" response. Thus, both the enzyme concentration and the assay time play important roles in the assay performance. For ATChE used in the Ellman's assay, if its concentration were too high, higher concentration of parathion-methyl would be needed to inhibit its activity and lead to poor sensitivity; if the ATChE concentration were too low, the blank color signal (no incubation with parathion methyl) could be too weak or take too long to reach a satisfactory color intensity. With an optimized ATChE concentration, the assay time needs to be carefully adjusted as well since the color could be weak if the reaction time is

Analyst Accepted Manuscript

View Article Online
DOI: 10.1039/D6AN00255B

too short, or the color could become saturated if the reaction time is too long. In this study, we systematically optimized these factors and the best assay performance was achieved with 0.25 μg/mL ATChE and a reaction time of 25 min. The details of optimization experiments are provided in the Supporting Information (Fig. S8-S11).

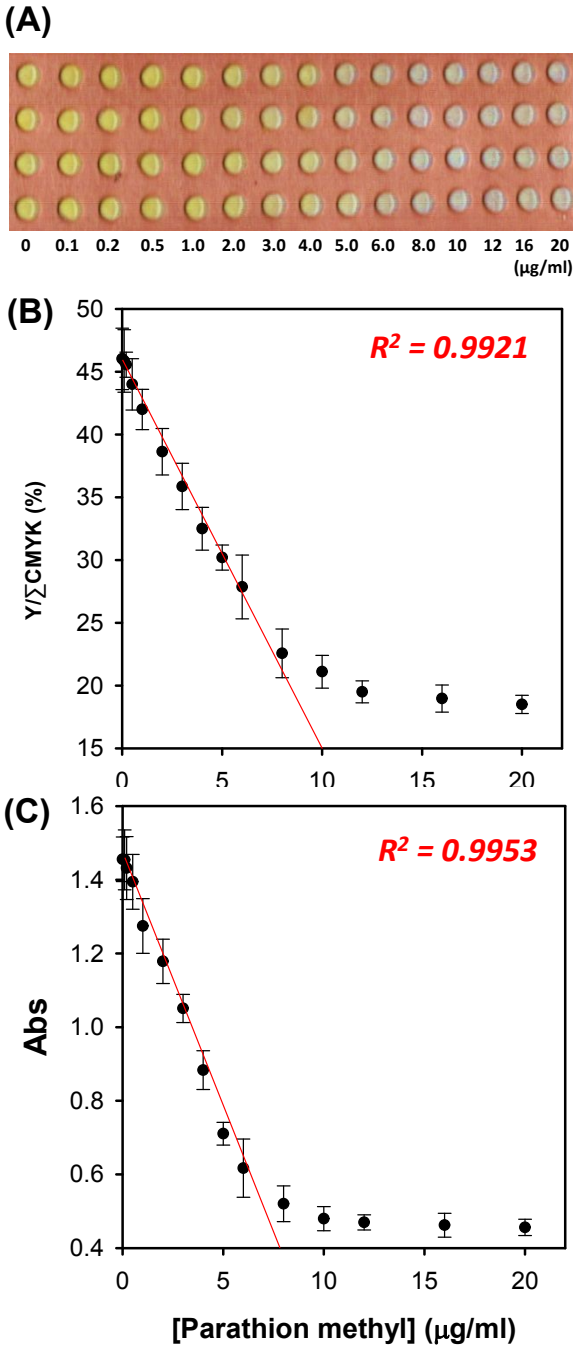

Fig. 7 (A) Wi-Fi scanned image of performing the Ellman's assay on hydrogel/paper disks (three repeats in 4 × 15 array) for the detection of parathion methyl (0-20 μg/mL). (B) Dependence of normalized Y value (Y/ΣCMYK) on the concentration of parathion methyl; the red solid line shows the best linear fit to the experimental data up to 6 μg/mL. (C) UV-vis absorbance measurements of the Ellman's assay solutions in the presence of 0 to 20 μg/mL of parathion methyl. The red line is also the best linear fit to the data from 0 to 6 μg/mL. The error bars in (B) and (C) were obtained from four repeating experiments.

Under the optimized condition, we performed Ellman's assay with the Wi-Fi scanning method after incubating ATChE with different concentrations of parathion methyl (0-20 μg/mL). Fig. 7 (A) shows the

Open Access Article. Published on 23 March 2026. Downloaded on 3/24/2026 12:02:26 AM.
This article is licensed under a Creative Commons Attribution-Non Commercial 3.0 Unported Licence.
Analyst Accepted Manuscript

View Article Online
DOI: 10.1039/D6AN00255B

scanned image of the detection results (three repeats in a 4 × 15 array format). It is clear to see that the higher concentration of parathion methyl leads to attenuated yellow intensity as a result of its inhibition effect on the ATChE activity. By analyzing the color intensities at each assay disk, the normalized yellow intensity (Y/ΣCMYK × 100%, ΣCMYK = C + M + Y + K) as the sensing response was plotted against the concentration of parathion methyl to generate the calibration curve. As shown in Fig. 7B, the normalized yellow intensity decreases monotonically before reaching a plateau at around 10 μg/mL; moreover, a linear response was found from 0 to 6 μg/mL (R^2 > 0.99). Fig. 7C is the calibration data obtained by conventional UV-vis spectrophotometry measurements (performing the Ellman's assay in microplate and using a plate reader to measure the absorbance), which has a similar "saturation" level (> 10 μg/mL) and a linear response range (0-6 μg/mL). More importantly, the LOD values of parathion methyl determined from the two linear regression fits in Fig. 6B and Fig. 6C are close to each other, i.e., 0.34 ± 0.12 μg/mL and 0.25 ± 0.10 μg/mL, respectively, indicating that the sensing performance of the two methods are very similar. Such a sensing performance is better than the quantitative results obtained by smartphone imaging in terms of both LOD and R^2 value of the linear fit (Fig. S14 in the Supplementary Information), and comparable with previously reported colorimetric sensors based on the Ellman's assay for the quantitation of parathion methyl, for which the LODs are from ng/mL to μg/mL.[49-50]

Table 1 Detection results of spiked parathion methyl in drinking water with both Wi-Fi scanning and traditional spectrophotometry methods.

[parathion methyl] $_{\text{added}}$ **(μg/mL)**	**[parathion methyl]** $_{\text{abs}}$ **(μg/mL)**	**[parathion methyl]** $_{\text{scanning}}$ **(μg/mL)**
0.0	Not detected	Not detected
2.0	1.89 ± 0.08 (90% to 99%*)	2.07 ± 0.11 (98% to 109%*)
5.0	5.15± 0.12 (101% to 106%*)	4.91 ± 0.19 (94% to 102%*)

*Recovery rates (100% × [Parathion methyl] determined / ([Parathion methyl] added)

To further compare the sensing performance, drinking water (tap water) spiked with two different concentrations of parathion methyl (0, 2.0 and 5.0 μg/mL) were tested by quantifying the results of Ellman's assays with the UV-vis spectrophotometry and the Wi-Fi scanning method. As presented in Table 1, the determined concentrations of parathion methyl ([parathion methyl]$_{abs}$ and [parathion methyl]$_{scanning}$) are both close to the spiked concentration of parathion methyl, i.e., [parathion methyl]$_{added}$, with satisfactory recovery rates (between 90 to 109%). More remarkably, it was found that after six months of storage under ambient conditions (room temperature), the hydrogel-paper disks still exhibit similar sensing performance (Fig. S16 in the Supplementary Information).

2.4. Comparison with other portable analytical systems and future perspectives

Nowadays, smartphones have become a popular imaging tool for colorimetric assay due to its intriguing advantages as described in the introduction section. However, the color information accuracy of smartphone image is often limited by several factors.[21,51] The most critical factor is uncontrolled illumination, as variations in surrounding light or the use of flash can cause glare, shadows, and uneven brightness, thereby compromising the accuracy of color analysis.[51-52] Perspective distortion is another factor of limitation, particularly when the objectives are not perfectly parallel or they have different focal distance to the camera lens.[16, 53] To address these issues, a range of hardware accessories, including dark boxes, convex lenses, and 3D-printed camera holders have been explored to standardize the imaging condition of smartphones and improve the color analysis accuracy.[16] In contrast, with a linear image sensor (typically a CCD or contact image sensor), built-in uniform light source (LED) and a cover lid, flatbed scanners have

Open Access Article. Published on 23 March 2026. Downloaded on 3/24/2026 12:02:26 AM.
This article is licensed under a Creative Commons Attribution-Non Commercial 3.0 Unported Licence.
Analyst Accepted Manuscript

View Article Online
DOI: 10.1039/D6AN00255B

highly reproducible imaging conditions; more importantly, the images obtained by scanners are not affected by ambient lights and perspective distortion (fixed focal distance across the entire scan area), which result in more consistent resolution and highly accurate color information across the entire image. Besides the conventional office scanner, the commercially available handheld Wi-Fi scanners further promoted their use as better alternatives of smartphones for reading PON tests (performing on-site colorimetric assays).

Compared to our previous study, where the anthocyanin pre-loaded hydrogel-paper disks were assembled onto a hydrophobic substrate (achieved by pre-treatment with 0.2% OTS/hexane solution) and merely used as a pH test strip,[34] the hydrogel-paper disk array developed in this work exhibits significant improvements and advantages. Firstly, the preparation of empty hydrogel/paper disks not only simplifies the fabrication process, but also allows for much broader applications (can be loaded with any colorimetric reagents, and are applicable for both enzymatic and chemical assays). Moreover, by simply assembling the paper disks on a commercial hydrophobic tape (no additional surface modification steps), a detection array of desired pattern and number of reaction zones can be readily obtained; the long shelf-life (> 6 months) also makes it possible for large-scale production and to be used as an economic alternative of conventional microplates for multiplex and high-throughput colorimetric detections (the 4 × 15 array testing results displayed in Figure 7A are close to the testing capacity of a 96-well microplate). We have demonstrated that the quantitation results of this new portable analytical system (Wi-Fi scanning + hydrogel-paper disk array) are comparable to conventional spectrophotometric measurements and smartphone analysis, which augments its great potential for practical use. In addition, a web-based mobile app (*ChromaDetect*) was developed in this study, which allow robust and convenient quantitative color analysis using smartphones, pads, and laptops compared to conventional software analysis using only computers (e.g., photoshop or Image J).

It should be noted that for practical application, the sample volume could have complex impacts on hydrogel-filter paper sensing platform (e.g., it directly controls the amounts of reagents/analytes used for each detection, evaporation could lead to dramatically increased local concentration of colorimetric reagents, the enzyme activity could be limited if the diffusion or capillary flow is too slow, insufficient or excess volume may result in uneven reagent distribution or “coffee ring” effect), which should be optimized for specific colorimetric assay by considering both technical and economic factors.

By and large, we expect such a digitized, Wi-Fi scanning platform could be expanded to a board range of colorimetric assays, such as nanoparticles based colorimetric assays and colorimetric immunoassays (with nanoparticles, labelled biorecognition element or substrate as pre-loading reagents). In addition to agarose films, the performance of this new platform when applied to specific colorimetric assay could be further enhanced by investigating the most suitable hydrogel material (alginate, chitosan, gelatin, etc.). The quality of scanned image can be further improved with less curved objective (e.g., smaller liquid volume), adjustable device to minimize the scanning space above the liquid drop, as well as more advanced portable scanners with higher resolution or intelligent scanning options (e.g., multi-direction and multi-mode scanning).

It is also anticipated to convert this portable, low-cost, user-friendly platform into commercially available PON devices, which will provide an alternative to laboratory-based spectroscopic method and greatly enhance the accessibility of quantitative colorimetric analysis in resource-limited settings or remote areas. Its robustness, scalability and ease of use will not only advance the analytical sciences (e.g., facilitating rapid field testing, environmental monitoring, and on-site diagnostics), but also generate broad societal benefits by supporting public health, food safety, and environmental protection initiatives. To achieve this goal, the long-term stability of the hydrogel-paper disk array (with or without preloaded colorimetric reagents) will also be evaluated (which is undergoing in our laboratory).

Open Access Article. Published on 23 March 2026. Downloaded on 3/24/2026 12:02:26 AM.
This article is licensed under a Creative Commons Attribution-NonCommercial 3.0 Unported Licence.
Analyst Accepted Manuscript

View Article Online
DOI: 10.1039/D6AN00255B

Open Access Article. Published on 23 March 2026. Downloaded on 3/24/2026 12:02:26 AM.
This article is licensed under a Creative Commons Attribution-Non Commercial 3.0 Unported Licence.

Analyst Accepted Manuscript

3. Conclusion

In this study, we have developed a portable PON platform that allow multiplexed, convenient, and quantitative analysis by using a disposable detection array made of hydrogel-filter paper mini-disk, a handheld Wi-Fi scanner to capture the resulting image, and a customized app for analyzing the color information (based on either RGB or CMYK color spaces). Its performance has been thoroughly validated with two colorimetric assays: the pH-differential colorimetric assay for anthocyanin and the Ellman's assay for parathion methyl. It was demonstrated that the quantitation results (e.g., response ranges, LODs, real sample detection) obtained with the Wi-Fi scanning platform is comparable with the conventional spectrophotometric measurements, indicating its reliability and feasibility for practical applications (either on-site chemical analysis or point-of-care medical diagnosis).

4. Experimental section

4.1 Materials and reagents

Agarose (low-EEO/multi-purpose, molecular biology grade, Fisher BioReagents), HCl (37%, USLI grade, GEM Microelectronic Materials, Nevada, AZ), NaOH (beads, ≥ 97.0%, ACS, VWR Chemicals BDH), cyanidin 3-O-glucoside chloride (Cy3G) standard (98% HPLC purity, Aobious Inc., Gloucester, MA), parathion methyl (analytical standard, Sigma-Aldrich, St. Louis, MO), acetylcholine chloride (ATCh,≥99% TLC, Sigma-Aldrich, St. Louis, MO), 5,5'-dithio-bis-(2-nitrobenzoic acid) (DTNB, ≥ 98%, Sigma-Aldrich, St. Louis, MO), acetylcholinesterase (ATChE, Sigma-Aldrich, St. Louis, MO), glycerol (ACS reagent ≥ 99.5%, Sigma-Aldrich, St. Louis, MO), ethanol (95%, Commercial Alcohols, Toronto, ON), disodium hydrogen phosphate heptahydrate ($Na_2HPO_4{\cdot}7H_2O$, Caledon Laboratories Ltd, Georgetown, ON), sodium dihydrogen phosphate monohydrate ($NaH_2PO_4{\cdot}H_2O$, Caledon Laboratories Ltd, Georgetown, ON), sodium acetate (CH_3COONa, ACS reagent ≥ 99.0%, Sigma-Aldrich, St. Louis, MO) and acetic acid (CH3COOH, ≥ 99.0%, Sigma-Aldrich, St. Louis, MO) were used as received unless otherwise noted. All beverage samples were provided by Laca Biotech Inc. and tested as received (except for dilution when needed). Deionized water (18.2 MΩ/cm) used throughout all experiments to prepare standard solutions and samples was produced freshly with a Barnstead EasyPure UV/UF compact water system (Dubuque, IA). Double-sided tape was purchased from Intertape Polymer Group. Grade-3 filter paper was obtained from Cytiva (Marlborough, MA).

Anthocyanin (Cy3G) stock solution: 1.0 mg/mL stock solution of Cy3G was prepared with DI water and stored at 4 °C before use. Acetylcholinesterase (ATChE) stock: 1.0 mg/mL stock solution (10 µL aliquots to avoid freeze-thaw cycles) was prepared by using sterile (via 0.2 µm filter) 0.1 M PB buffer containing 10% glycerol; the aliquots were stored at -20 °C before use. Parathion methyl stock solution: 1.0 mg/mL stock solution was prepared with ethanol and stored at 4 °C. The pH 1.0 solution was prepared with 1.0 M HCl, the pH 4.5 buffer was prepared with CH_3COONa and CH_3COOH (adjusted with 0.1 M HCl or 0.1 M NaOH), and the pH 7.5 PB buffer (0.1 and 0.01 M) was prepared with $NaH_2PO_4{\cdot}H_2O$ and $Na_2HPO_4{\cdot}7H_2O$ (pH adjusted with 0.1 M HCl or 0.1 M NaOH).

4.2. Fabrication of hydrogel-paper disk assay

The hydrogel-coated filter paper was prepared by dissolving agarose powder in 70 °C water (w/v = 5%) and stirred for at least 15 min to obtain a clear, homogeneous solution (all agarose dissolved).[34] Subsequently, the agarose solution was immediately poured onto a piece of grade-3 filter paper placed inside the lid of a plastic Petri dish, and the bottom of the Petri dish was pressed on top. To control the

View Article Online
DOI: 10.1039/D6AN00255B

thickness of agarose film, double-sided tapes were positioned between the dish bottom and lid to separate them by ~0.75 mm. After pressing for at least 30 min, the hydrogel-coated filter paper was taken out, dried overnight, and was stored at room temperature before use.

To assemble the mini-disk array, the hydrogel-coated filter paper was cut into 5 mm diameter disks by using Explore 4 smart cutting machine (Cricut, Inc., South Jordan, Utah), The paper disk were then aligned and stick to double-sided tape (the other side of tape was stick to a solid substrate) with appropriate distance between each other (> 0.5 cm).

4.3. Colorimetric assay procedures for anthocyanin and parathion methyl

Anthocyanin (Cy3G) detection (Wi-Fi scanning): The pH 1.0 solution and the pH 4.5 buffer of 20 μL was loaded to the hydrogel-paper disk array, dried overnight, and stored at ambient environment before use. For the quantitation, 20 μL Cy3G solution of different concentrations (diluted from the 1.0 mg/mL stock solution with water, from 0 to 120 mg/L) was added to the pH 1.0 solution and the pH 4.5 buffer pre-loaded on the disk. After observing the color change, a mini-handheld iScan portable scanner (Brand: Loomza) was used to capture the image of detection results (JPG format), followed by quantitative analysis with the customized app (to the determine normalized R value) and construct the calibration curve.

Anthocyanin (Cy3G) detection (UV-vis): The 1.0 mg/mL stock solution of Cy3G was diluted to different concentrations (0 to 200 μg/mL) with pH 1.0 solution and the pH 4.5 buffer. For each diluted Cy3G solution, transfer 1.0 mL to a glass cuvette and measured its spectrum with an Ocean Optics QE65000 spectrophotometer equipped with a DU-2000-BAL deuterium and tungsten lamp and a 600 μm SR optical fiber probe (Winter Park, FL). The absorbance at the maximum wavelength of each diluted Cy3G solution (512 nm) was quantitatively analyzed with the pH differential method.

Parathion methyl detection (Wi-Fi scanning): 20 μL solution of the mixture of ATCh (2.5 mg/mL) and DTNB (1.0 mg/mL) was loaded to the hydrogel-paper disk array, dried overnight, and stored at ambient environment before use. For parathion methyl detection, the 1.0 mg/mL stock solution was diluted with 10 mM PB buffer to desired concentrations (0-50 μg/mL). For the ATChE inhibition assay, 1 μL of ATChE aliquot (1 mg/mL, stored at -20 °C) was first diluted by 0.01 M PBS buffer to 150 μL; subsequently, 4 μL of diluted ATChE was added to 100 μL of parathion methyl of different concentrations and incubated at 37 °C for 30 min (the final ATChE concentration is 250 ng/mL). Subsequently, 20 μL of incubation solution was added to ATCh/DTNB preloaded disk; after waiting for 25 min, we use the handheld Wi-Fi scanner (iScan) to capture the assay image, followed by quantitative analysis with the app (to determine normalized Y values).

Parathion methyl detection (UV-vis): 1.0 mg/mL parathion methyl stock solution was diluted with 10 mM PB buffer to desired concentrations (0-50 μg/mL). For ATChE inhibition, 1 μL of ATChE aliquot (1 mg/mL, stored at -20 °C) was first diluted by 0.01 M PB buffer to 150 μL; subsequently, 4 μL of the diluted ATChE was added to 200 μL of parathion methyl of different concentrations and incubated at 37 °C for 30 min (the final ATChE concentration is 0.1 μg/mL). After incubation, 20 μL of the binary solution of ATCh (2.5 mg/mL) and DTNB (1.0 mg/mL) was added and then waiting for 25 min before the absorbance measurement. To obtain the spectrum and determine the maximum absorbance wavelength, the reaction solution was transferred to a cuvette and scanned with the same spectrophotometer noted above. For quantitative detection, each incubation solution was prepared in a well on a *fisherbrand* microplate (Fisher Scientific, Hampton, NH); after adding ATCh/DTNB mixture, a Tecan Infinite 200 Pro Microplate Reader (Männedorf, Switzerland) was used to measure the absorbance at the maximum wavelength (412 nm).

Acknowledgement

Open Access Article. Published on 23 March 2026. Downloaded on 3/24/2026 12:02:26 AM.
This article is licensed under a Creative Commons Attribution-Non Commercial 3.0 Unported Licence.
Analyst Accepted Manuscript

View Article Online
DOI: 10.1039/D6AN00255B

Open Access Article. Published on 23 March 2026. Downloaded on 3/24/2026 12:02:26 AM.
This article is licensed under a Creative Commons Attribution-NonCommercial 3.0 Unported Licence.

Analyst Accepted Manuscript

This work was funded by the Natural Science and Engineering Research Council (NSERC) of Canada through a Discovery Grant (PI: H.Y.) and an Alliance International Catalyst Grant (PIs: H.Y.; A.T.). This work also made use of the 4D LABS shared facilities supported by the Canada Foundation for Innovation (CFI), British Columbia Knowledge Development Fund (BCKDF), Western Economic Diversification Canada (WD) and Simon Fraser University (SFU). P.P. would like to thank the Government of Canada for the SEED (Scholarships and Educational Exchanges for Development) scholarship which supported his stay at SFU as a visiting graduate student. We also thank Shirin Yazdani for her help in preparing some of the procedure diagrams in the Supporting Information.

Supporting information

Description of the design and function of the color analysis app; the fabrication and detection procedure of hydrogel-coated filter paper; the influence of using scanning box on the imaging results; optimization of the two colorimetric assays performed with the Wi-Fi scanning method and conventional UV/Vis spectrophotometric measurements; additional photos and quantitation results of real samples; the original codes for the ChromaDetect app.

References

1. Z. Jin, W. Yim, M. Retout, E. Housel, W. Zhong, J. Zhou, M. S. Strano and J. V. Jokerst, *Chem. Soc. Rev.*, 2024, **53**, 7681–7741.
2. C. V. Sapan, R. L. Lundblad and N. C. Price, *Biotechnol. Appl. Biochem.*, 1999, **29**, 99–108.
3. Y. Wu, J. Feng, G. Hu, E. Zhang and H.-H. Yu, *Sensors*, 2023, **23**, 2749.
4. Y. K. Shrestha and S. K. Shrestha, in *Advances in Colorimetry*, IntechOpen, 2023.
5. J. Yang, X. Wang, Y. Sun, B. Chen, F. Hu, C. Guo and T. Yang, *Biosensors*, 2022, **13**, 29.
6. W. Zhao, M. A. Brook and Y. Li, *ChemBioChem*, 2008, **9**, 2363–2371.
7. Y. Lee, I. Haizan, S. B. Sim and J.-H. Choi, *Biosensors*, 2025, **15**, 362.
8. Y. Song, W. Wei and X. Qu, *Adv. Mater.*, 2011, **23**, 4215–4236.
9. A. P. V. S., P. Joseph, K. D. S. C. G., S. Lakshmanan, T. Kinoshita and S. Muthusamy, *Mater. Sci. Eng. C*, 2017, **78**, 1231–1245.
10. A. Ko and C. Liao, *Anal. Methods*, 2023, **15**, 4377–4404.
11. F. Di Nardo, M. Chiarello, S. Cavalera, C. Baggiani and L. Anfossi, *Sensors*, 2021, **21**, 5185.
12. W. C. Mak, V. Beni and A. P. F. Turner, *TrAC, Trends Anal. Chem.*, 2016, **79**, 297–305.
13. V. Kumar and K. D. Gill, in *Basic Concepts in Clinical Biochemistry: A Practical Guide*, Springer, 2018, pp. 17–20.
14. G. A. Parker and D. Boltz, in *Modern Methods of Geochemical Analysis*, Springer, 1971, pp. 97–126.
15. B. R. Sun, A. G. Zhou, X. Li and H.-Z. Yu, *ACS Sens.*, 2021, **6**, 1731–1744.
16. R. Deng, X. Chao, H. Li, X. Li, Z. Yang and H.-Z. Yu, *Analyst*, 2023, **148**, 735–741.
17. X. Li, F. Yang, J. X. Wong and H.-Z. Yu, *Anal. Chem.*, 2017, **89**, 8908–8916.
18. J. Guo, J. X. Wong, C. Cui, X. Li and H.-Z. Yu, *Analyst*, 2015, **140**, 5518–5525.
19. Y. Fan, J. Li, Y. Guo, L. Xie and G. Zhang, *Measurement*, 2021, **171**, 108829.

View Article Online
DOI: 10.1039/D6AN00255B

20. A. Roda, E. Michelini, M. Zangheri, M. Di Fusco, D. Calabria and P. Simoni, *TrAC, Trends Anal. Chem.*, 2016, **79**, 317–325.

21. D. V. Baker, J. Bernal-Escalante, C. Traaseth, Y. Wang, M. V. Tran, S. Keenan and W. R. Algar, *Lab Chip*, 2025, DOI: 10.1039/XXXXXXX.

22. S. Qian, Y. Cui, Z. Cai and L. Li, *Biosens. Bioelectron.*, 2022, **11**, 100173.

23. S. Kanchi, M. I. Sabela, P. S. Mdluli and K. Bisetty, *Biosens. Bioelectron.*, 2018, **102**, 136–149.

24. L. Shen, J. A. Hagen and I. Papautsky, *Lab Chip*, 2012, **12**, 4240–4243.

25. J. Li, M. L. O'Neill, C. Pattison, J. H. Zhou, J. M. Ito, C. S. Wong, H.-Z. Yu and N. Merbouh, *J. Chem. Educ.*, 2023, **100**, 1234–1242.

26. J. Wang, L. Zhang, X. Li, X. Zhang and H.-Z. Yu, *RSC Adv.*, 2019, **9**, 23267–23275.

27. J. R. Askim and K. S. Suslick, *Anal. Chem.*, 2015, **87**, 7810–7816.

28. G. Sriram, M. P. Bhat, P. Patil, U. T. Uthappa, H.-Y. Jung, T. Altalhi, T. Kumeria, T. M. Aminabhavi, R. K. Pai and M. D. Kurkuri, *TrAC, Trends Anal. Chem.*, 2017, **93**, 212–227.

29. T. Kant, K. Shrivas, A. Tejwani, K. Tandey, A. Sharma and S. Gupta, *Nanoscale*, 2023, **15**, 19016–19038.

30. M. C. Carneiro, L. R. Rodrigues, F. T. Moreira and M. G. F. Sales, *Sensors*, 2022, **22**, 3221.

31. K. Fan, X. Wang, H. Gao, G. Han, L. Zhou and S. Fang, *Anal. Methods*, 2020, **12**, 1561-1566.

32. T. Choleva, C. Matiaki and D. L. Giokas, *Sens. Actuators, B*, 2023, **386**, 133729.

33. L. Zhang, H. Kwok, X. Li and H.-Z. Yu, *ACS Appl. Mater. Interfaces*, 2017, **9**, 39728–39735.

34. M. Leung, L. Zhang, X. Li and H.-Z. Yu, *Anal. Chem.*, 2024, **96**, 15808–15815.

35. V. J. Liebich, O. Avrutina, J. Habermann, L. M. Hillscher, M. Langhans, T. Meckel, M. Biesalski and H. Kolmar, *Biomacromolecules*, 2021, **22**, 2954–2962.

36. J. Tavakoli and Y. Tang, *Polymers*, 2017, **9**, 364.

37. W. Cheng, X. Wu, Y. Zhang, D. Wu, L. Meng, Y. Chen and X. Tang, *Trends Food Sci. Technol.*, 2022, **129**, 244–257.

38. S. Huang, G. Wang, H. Lin, Y. Xiong, X. Liu and H. Li, *Sens. Actuators Rep.*, 2021, **3**, 100049.

39. https://www.bhphotovideo.com/lit_files/255716.pdf, accessed March 4, 2026.

40. R. Mattioli, A. Francioso, L. Mosca and P. Silva, Molecules, 2020, 25, 3809.

41. E. Sondheimer and Z. Kertesz, *Anal. Chem.*, 1948, **20**, 245–248.

42. J. Lee, R. W. Durst and R. E. Wrolstad, *J. AOAC Int.*, 2005, **88**, 1269–1278.

43. B. Fallico, E. Arena, E. Chiappara and G. Ballistreri, *Food Addit. Contam.*, 2010, **27**, 201–211.

44. F. L. Edwards and P. B. Tchounwou, *Int. J. Environ. Res. Public Health*, 2005, **2**, 430–441.

45. S. Garcia, A. Abu-Qare, W. Meeker-O'Connell, A. Borton and M. Abou-Donia, *J. Toxicol. Environ. Health, Part B*, 2003, **6**, 185–210.

46. P. S. Jaglan, R. B. March, T. R. Fukuto and F. A. Gunther, *J. Agric. Food Chem.*, 1970, **18**, 809–813.

47. I. Che Sulaiman, B. Chieng, M. Osman, K. Ong, J. Rashid, W. M. Wan Yunus, S. Noor, N. Kasim, N. Halim and A. Mohamad, *Microchim. Acta*, 2020, **187**, 131.

48. F. Worek, P. Eyer and H. Thiermann, *Drug Test. Anal.*, 2012, **4**, 282–291.

49. M. Bhattu, M. Verma and D. Kathuria, *Anal. Methods*, 2021, **13**, 4390–4428.

50. X. Meng, C. W. Schultz, C. Cui, X. Li and H.-Z. Yu, *Sens. Actuators, B*, 2015, **215**, 577–583.

51. X. Bao, S. Jiang, Y. Wang, M. Yu and J. Han, *Analyst*, 2018, **143**, 1387–1395.

Open Access Article. Published on 23 March 2026. Downloaded on 3/24/2026 12:02:26 AM.
This article is licensed under a Creative Commons Attribution-NonCommercial 3.0 Unported Licence.

Analyst Accepted Manuscript

View Article Online
DOI: 10.1039/D6AN00255B

52. S. Dutta, *TrAC, Trends Anal. Chem.*, 2019, **110**, 393–400.

53. G. Zhang, S. Song, J. Panescu, N. Shapiro, K. C. Dannemiller and R. Qin, *PLoS One*, 2023, **18**, e0287099.

Open Access Article. Published on 23 March 2026. Downloaded on 3/24/2026 12:02:26 AM.
This article is licensed under a Creative Commons Attribution-Non Commercial 3.0 Unported Licence.

Analyst Accepted Manuscript

View Article Online
DOI: 10.1039/D6AN00255B

Open Access Article. Published on 23 March 2026. Downloaded on 3/24/2026 12:02:26 AM.
This article is licensed under a Creative Commons Attribution-NonCommercial 3.0 Unported Licence.

Data availability statement

for

Quantitative Analysis of Colorimetric Hydrogel/Paper Disk Arrays with a Handheld Wi-Fi Scanner

Lin Qi,[†a] Pitipat Parittothok,[†ab] Sophia Sun,[a] Jakrapop Wongwiwat,[b] Aluck Thipayarat,[c] Wanida Laiwattanapaisal,[d] and Hua-Zhong Yu*[ad]

[a] *Department of Chemistry, Simon Fraser University, Burnaby, British Columbia V5A 1S6, Canada*

[b] *Department of Mechanical Engineering, King Mongkut's University of Technology Thonburi, Bangkok 10140, Thailand*

[c] *Department Food Engineering, King Mongkut's University of Technology Thonburi, Bangkok 10140, Thailand*

[d] *Department of Clinical Chemistry, Chulalongkorn University, Bangkok 10330, Thailand*

* Corresponding author. E-mail: hogan_yu@sfu.ca

[†] These authors contributed equally to the work.

The authors confirm that the data supporting the findings of this study are available within the article and its Supplementary Information (SI).

Analyst Accepted Manuscript